Magnetic Acceleration and Collimation of Gamma-Ray Burst Jets

Arieh Königl

Department of Astronomy & Astrophysics, University of Chicago, 5640 S. Ellis Ave., Chicago, IL 60637, U.S.A.

Abstract. Exact semianalytic solutions for GRB outflows were recently derived using the equations of special-relativistic ideal MHD (see the contribution by Vlahakis & Königl for a summary). This contribution focuses on the implications of these results to various modeling and observational issues in GRB sources, including the baryon loading problem, polarization measurements of the prompt and reverse-shock emission, and the possible existence of a two-component outflow.

1. MAGNETIC DRIVING OF GRB OUTFLOWS

Gamma-ray burst (GRB) outflows are likely powered by the extraction of rotational energy from a newly formed stellar-mass black hole or neutron star, or from a surrounding debris disk established in the course of the central object's formation [e.g., 15]. Magnetic fields threading the central object or disk provide the most plausible means of extracting the inferred amount of energy on the timescale of the burst; they can also guide, collimate, and accelerate the flow [see 20, and references therein]. This picture is supported by a recent measurement of a high ($80 \pm 20\%$) linear polarization in the prompt γ-ray emission from GRB 021206 [5], which can be plausibly interpreted in terms of a large-scale magnetic field advected from the origin [e.g., 11] and is consistent with magnetic driving by an ordered field that threads the source. Although purely hydrodynamic driving powered by neutrino emission or magnetic field dissipation at the source can probably be ruled out [e.g., 8, 6], thermal effects may nonetheless dominate the initial acceleration of magnetic jets [e.g., 16, 20].[1]

Motivated by the above considerations, Vlahakis & Königl [21, 22, hereafter VK03a and VK03b, respectively] constructed a general formalism for special-relativistic ideal MHD, allowing for the presence of a baryonic component as well as of a "hot" electron-positron/radiation component that can dominate the pressure. They showed how one can derive exact semianalytic solutions for axisymmetric outflows under the assumption of radial self-similarity and presented illustrative results for representative GRB parameters. Vlahakis, Peng, & Königl [23, hereafter VPK03] further generalized this scheme by obtaining solutions for initially neutron-rich outflows, which they used to address the baryon loading problem in GRB source models. A general description of the formal-

[1] It has also been argued [e.g., 9] that electromagnetic energy dissipation could contribute to the conversion of Poynting energy into kinetic energy throughout the acceleration region of such flows.

ism and of the derived solutions is given in Vlahakis & Königl's contribution in these Proceedings. The present contribution provides a brief overview of the main results and focuses on their observational implications.

2. RELATIVISTIC MHD SOLUTIONS

The initial (subscript i) magnetic field amplitude can be inferred from an estimate of the injected energy, $\mathscr{E}_{\rm i}$ = (Poynting flux) $\times$ (surface area) $\times$ (burst duration). In a disk geometry [with initial cylindrical radius $\varpi_{\rm i}$ and radial width $(\Delta\varpi)_{\rm i}$], $\mathscr{E}_{\rm i} \approx cE_{\rm i}B_{\phi,{\rm i}}\varpi_{\rm i}(\Delta\varpi)_{\rm i}\Delta t$, where the electric field is given by $E = B_{\rm p}V_\phi/c - B_\phi V_p/c$ (with the subscripts p and ϕ denoting the poloidal and azimuthal components, respectively). For characteristic parameter values [$\mathscr{E}_{\rm i} \approx 10^{52}$ ergs, $\varpi_{\rm i} \sim (\Delta\varpi)_{\rm i} \approx 10^6$ cm, $\Delta t \approx 10$ s], one obtains $B_{\rm i} \sim 10^{14} - 10^{15}$ G. This field is most plausibly generated by differential-rotation amplification of a much weaker poloidal field component that originally threads the source.

If $|B_{\rm p,i}/B_{\phi,{\rm i}}| > 1$, a *trans-Alfvénic* outflow is produced, whereas if $|B_{\phi,{\rm i}}/B_{\rm p,i}| > 1$, the outflow is *super-Alfvénic* from the start. The latter situation may correspond to amplified toroidal flux loops that have been disconnected by magnetic reconnection and escape from the disk surface in a nonsteady fashion. Exact solutions for these two situations were derived in VK03a and VK03b, respectively. It was demonstrated that, in either case, Poynting flux-dominated jets can transform $\gtrsim 50\%$ of their magnetic energy into baryon kinetic energy (with $E_{\rm K} \sim 10^{51}$ ergs and terminal Lorentz factors $\gamma_\infty \sim 10^2 - 10^3$). If relativistic e^+e^- pairs and radiation dominate the initial enthalpy, then a thermal acceleration zone develops at the base of the flow and remains dominant until the specific enthalpy drops below $\sim c^2$, at which point magnetic acceleration takes over. In contrast to the trans-Alfvénic solutions, part of the enthalpy flux in the super-Alfvénic flows is transformed into Poynting flux during the thermal acceleration phase. Furthermore, the subsequent, magnetically dominated acceleration in these flows can be significantly less rapid than in the trans-Alfvénic case.

The derived solutions have a free parameter, F, which controls the distribution of the poloidal current $I = c\varpi B_\phi/2$. For $F > 1$ the flow is in the current-carrying regime, with the poloidal current density being antiparallel to the magnetic field. In this case the current tends to zero as the symmetry axis is approached, so such solutions should provide a good representation of the conditions near the axis of a highly collimated flow. Conversely, solutions with $F < 1$ correspond to the return-current regime (in which the poloidal current density is parallel to the field) and are most suitable at larger cylindrical distances. Although the detailed global current distribution cannot be modeled using the self-similarity approach, one can nevertheless generate "hybrid" flow configurations that combine a current-carrying solution for low values of ϖ and a return-current solution for high values of ϖ (see Fig. 1 below for an example). Initially Poynting-dominated flows that attain a rough equipartition between the kinetic and Poynting energy fluxes at large distances from the origin have F close to 1. When $F > 1$ the Lorentz force can collimate the flow to cylindrical asymptotics. For $F < 1$ the collimation is weaker and the flow only reaches conical asymptotics; however, the acceleration is more efficient in this case in that a larger fraction of the Poynting flux is converted into kinetic energy.

3. IMPLICATIONS TO THE BARYON LOADING PROBLEM

As an illustration of the unique properties of the relativistic MHD solutions, consider the ramifications of a hydromagnetic jet model to the baryon loading problem in GRB outflows. The apparent difficulty stems from a comparison between the estimated mass of protons in the jet, $M_{\rm proton} = 3\times10^{-6}(E_{\rm K}/10^{51}\ {\rm ergs})(\gamma_\infty/200)^{-1}\ M_\odot$, and the minimum mass of the debris disk from which the jet is thought to originate, obtained under the assumption that at most $\sim 10\%$ of the disk gravitational potential energy could be converted into outflow kinetic energy. This comparison implies that the outflow can comprise at most $\sim 10^{-4}$ of the disk mass, whereas disk outflow models that utilize a large fraction of the disk potential energy typically also entail substantial mass loading. One approach to this issue has been to postulate that the outflow emerges along magnetic field lines that thread the black-hole event horizon and not the disk, but then the converse problem — how to avoid having too few baryons — must be addressed [e.g., 13]. A possible resolution of the problem in the context of disk-fed jet models was proposed in [10], where it was noted that such outflows are expected to be neutron-rich [neutron/proton ratios as high as ${\rm n/p}\sim 20-30$; e.g., 18, 2, 23]. Since only the charged outflow component couples to the electromagnetic field, the neutrons could potentially decouple from the protons before the latter attain their terminal Lorentz factor. In this picture, the inferred value of $M_{\rm proton}$ may represent only a small fraction of the total baryonic mass ejected from the disk, which would alleviate the loading problem. However, it can be shown that, for purely hydrodynamic outflows, the Lorentz factor $\gamma_{\rm d}$ at decoupling is at least a few times 10^2 [e.g., 7, 2, 23]. This implies that $\gamma_{\rm d}/\gamma_\infty \sim 1$ and hence that the protons end up with only a small fraction of the injected energy, which is *not* a satisfactory resolution of the problem.

As demonstrated by VPK03, the incorporation of magnetic fields makes it possible to attain $\gamma_{\rm d} \ll \gamma_\infty$ and thereby reclaim the promise of the Fuller et al. proposal. They wrote down the equations of motion for the neutron component (which couples to the protons through a collisional drag) and for the charged component (incorporating protons and their neutralizing electrons as well as initially "hot" pairs and radiation), and simplified them by considering a well-coupled neutral/charged fluid for $\gamma \le \gamma_{\rm d}$ and only the charged fluid component for $\gamma > \gamma_{\rm d}$. The pre-decoupling region was described by a super-Alfvénic outflow solution. As noted in § 2, in this case part of the enthalpy flux is converted into Poynting flux during the initial thermal acceleration phase. This reduces the acceleration rate, so at the point of decoupling (when $V_{\rm proton} - V_{\rm neutron} \sim c$) the Lorentz factor is still comparatively low. The energy deposited into the Poynting flux is returned to the matter beyond the decoupling point as kinetic energy, thereby enhancing the acceleration efficiency of the proton component. The end result is a large $\gamma_\infty/\gamma_{\rm d}$ ratio *and* comparable terminal kinetic energies in the proton and neutron components, in clear contradistinction to the purely hydrodynamic solutions.

An illustrative solution is shown in Fig. 1.[2] The top panel shows the behavior of the

[2] In this example ${\rm n/p} = 30$, the pre-decoupling and post-decoupling regions correspond to the current-carrying ($F = 1.05$) and return-current ($F = 0.1$) regimes, respectively, and the flow collimates from an initial opening half-angle of 55° to $\theta_{\rm j} \approx 20^\circ$.

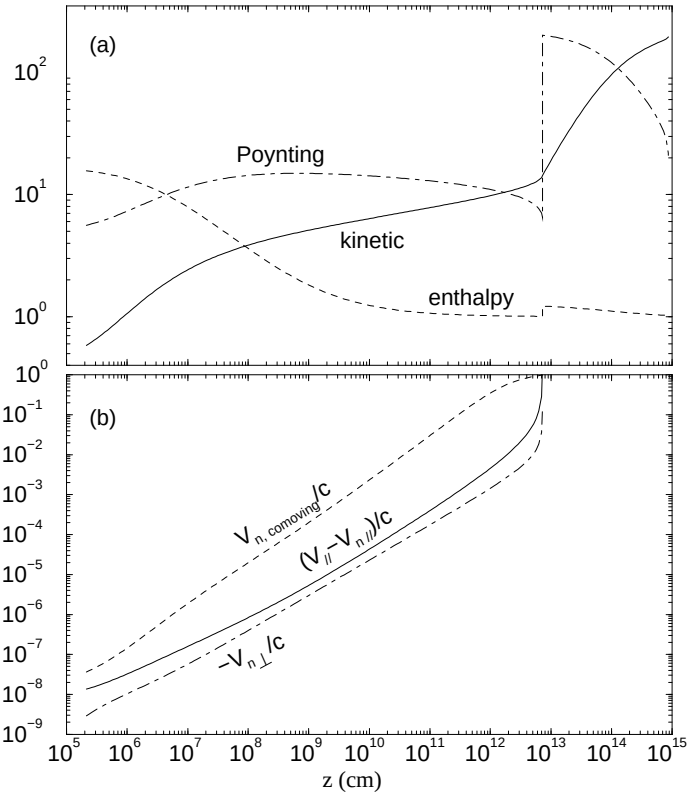

FIGURE 1. Illustrative relativistic-MHD solution of a neutron-rich outflow. (*a*) Components of the total energy flux, normalized by the mass flux $\times\, c^2$, as functions of height along a fiducial magnetic field line. The Poynting and enthalpy curves are discontinuous at the decoupling point, reflecting the decrease in the mass flux of field-coupled gas above that point. (*b*) Components of the proton–neutron drift velocity.

various components of the energy flux, corroborating the qualitative description given above. The thermal acceleration effectively terminates at a height $z \approx 10^9$ cm above the disk, and the neutrons decouple from the protons at $z_{\rm d} \approx 10^{13}$ cm, corresponding to $\gamma_{\rm d} \approx 15$. By the time of decoupling the neutrons have acquired $\sim 2/3$ of the injected energy, with the remainder residing predominantly in the electromagnetic field. The latter portion is then transferred with almost 100% efficiency into proton kinetic energy, so that, ultimately, the protons have $\gamma_\infty = 200$ and $E_{\rm K,proton} \approx 10^{51}$ ergs $\approx 0.5 E_{\rm K,neutron}$. The proton jet thus carries $\sim 1/3$ of the injected energy but only $\sim 3\%$ of the injected mass. The lower panel of Fig. 1 shows that, even though the decoupling in this case is initiated by the growth of the n–p drift velocity along the poloidal magnetic field, there is also a transverse drift component (induced by the ongoing magnetic collimation), which at the time of decoupling is $V_{\rm neutron,\perp} \sim 0.1c$.[3]

[3] The exact value of the angle between $\mathbf{V}_{\rm n}$ and $\mathbf{V}_{\rm p}$ at decoupling can only be obtained by solving the equations of motion without the "strong coupling" approximation adopted in the solution shown in Fig. 1.

4. ADDITIONAL IMPLICATIONS

Polarization — Magnetic driving of GRB outflows by large-scale, ordered magnetic fields would naturally lead to a large linear polarization P in the prompt γ-ray emission, and a high value of P is also predicted for the emission from the *reverse shock* (the "optical flash" and "radio flare") [12]. As shown in [11], in this picture the prompt emission may be expected to exhibit $P \sim 43\% - 61\%$ for typical values of the synchrotron-radiation spectral index, consistent with the observations of GRB 021206 [5]. The ordered field is also expected to induce measurable circular polarization [14].

Two-Component Outflow — The decoupled neutrons in a neutron-rich outflow will undergo β decay into protons at a distance $\sim 4 \times 10^{14}\,(\gamma_{\rm d}/15)$ cm. In contrast with the situation in purely hydrodynamic outflow models [17, 1], there may well be *no* interaction between the two decoupled components in the MHD case since their motions are not collinear (see Fig. 1*b*). The latter scenario thus gives rise to a 2-component outflow: an outer (wider) component (comprising the decoupled neutrons) that carries most of the energy and may be responsible (after the neutrons decay) for the bulk of the optical/radio afterglow, and an inner (narrower) component (comprising the original protons) that accounts for the prompt γ-rays and possibly also for much of the X-ray afterglow. A 2-component outflow of this type was inferred in GRB 030329 [3, 19]. A more detailed investigation of this scenario is currently under way. If $E_{\rm K,narrow} \lesssim E_{\rm K,wide}$ and $\theta_{\rm j,narrow}/\theta_{\rm j,wide} \lesssim 1/3$, this picture would make it possible to reconcile current inferences of the radiated γ-ray energy [e.g., 4] with internal-shock models.

REFERENCES

1. Beloborodov, A. M. 2003a, ApJ, 585, L19
2. _____. 2003b, ApJ, 588, 931
3. Berger, E., et al. 2003, Nature, 426, 154
4. Bloom, J. S., Frail, D., A., & Kulkarni, S. R. 2003, ApJ, 594, 674
5. Coburn, W., & Boggs, S. E. 2003, Nature, 423, 415
6. Daigne, F., & Mochkovitch, R. 2002, MNRAS, 336, 1271
7. Derishev, E. V., Kocharovsky, V. V., & Kocharovsky, Vl. V. 1999, ApJ, 521, 640
8. Di Matteo, T., Perna, R., & Narayan, R. 2002, ApJ, 579, 706
9. Drenkhahn, G., & Spruit, H. C. 2002, A&A, 391, 1141
10. Fuller, G. M., Pruet, J., & Abazajian, K. 2000, Phys. Rev. Lett., 85, 2673
11. Granot, J. 2003, ApJ, 596, L17
12. Granot, J., & Königl, A. 2003, ApJ, 594, L83
13. Levinson, A., & Eichler, D. 2003, ApJ, 594, L19
14. Matsumiya, M., & Ioka, K. 2003, ApJ, 595, L25
15. Mészáros, P. 2002, ARA&A, 40, 137
16. Mészáros, P., Laguna, P., & Rees, M. J. 1993, ApJ, 415, 181
17. Pruet, J., & Dalal, N. 2002, ApJ, 573, 770
18. Pruet, J., Woosley, S. E., & Hoffman, R. D. 2003, ApJ, 586, 1254
19. Sheth, K., et al. 2003, ApJ, 595, L33
20. Vlahakis, N., & Königl, A. 2001, ApJ, 563, L129
21. _____. 2003a, ApJ, 596, 1080 (VK03a)
22. _____. 2003b, ApJ, 596, 1104 (VK03b)
23. Vlahakis, N., Peng, F., & Königl, A. 2003, ApJ, 594, L23 (VPK03)